ZnO Nanoparticles Beaded Multiwalled Carbon Nanotubes

Y. Zhu[*], H. I. Elim [*], Y. L. Foo [**], S. Triparthy [**], W. T. Quek [*], W. Ji [*], J. Thong [***] and C. H. Sow [*]

[*]Department of Physics, National University of Singapore (NUS)
S12, 2 Science Drive 3, Singapore 117542, physowch@nus.edu.sg (C. H. Sow)
[**]Institute of Materials Research & Engineering, Singapore
[***]Department of Electrical and Computer Engineering, NUS, Singapore

ABSTRACT

In this work, we present a very simple technique to fabricate hybrid nanomaterial system comprising of ZnO nanobeads anchored onto the cylindrical body of CNTs. This is achieved simply by heating Zn coated CNTs on a hotplate in air. By directly changing the Zn coating duration and thus coating thickness, the average ZnO particle size and interparticle distance can be readily controlled. The obtained nanoparticle are characterized to be single crystalline, following hexagonal ZnO structures. Low temperature photoluminescence at 77K and temperature dependence studies have been carried out to explore the optical property of the ZnO nanoparticles on CNTs. Based on this ZnO/MWNTs hybrid system, an ultrafast nonlinear optical switching behavior is demonstrated and three-photon adsorption of ZnO nanoparticles is observed. By using the same synthesis process, ZnO nanoparticles have also been coated on CuO nanowires.

Keywords: ZnO, carbon nanotubes, hybrid material, nanoparticle, nonlinear absorption

1 INTRODUCTION

Nanoparticles, whose size is at the nanometer scale in all three dimensions, have attracted much attention due to their unique photonic, electronic, magnetic and catalytic properties [1]. Assembly of isotropic nanoparticles onto one-dimensional (1D) architectures represents an important step towards the integration of nanoparticles in nanodevices [2]. In particular, nanoparticles of one material can be assembled on a 1D nanostructure of a different material to form unique and interesting hybrid nanomaterial systems [3]. Recently, carbon nanotubes (CNTs) have been used as templates or scaffolds for the hybrid assembly of nanoparticles [4-10]. With their great hardness and toughness, CNTs keep their morphology and structure, even with high nanoparticle loadings. More importantly, some of these beaded CNT hybrid systems exhibit unique properties. For example, supercapacitances in RuO_2/CNT composite [11], diode-like rectification based on Co_3O_4 beaded CNTs [12], and improved optical limiting from Au and Ag coated CNTs [13], have been demonstrated.

As an important wide band-gap (3.37 eV) semiconductor with a large exciton binding energy (60 meV), ZnO has received widespread attention due to its excellent performance in electronics, optics, and photonics systems [14]. As two important building blocks in nanotechnology, ZnO nanoparticles and CNTs are rarely assembled as hybrid structures [15-18]. W. Sigmund *et al.* [15], and J. Park *et al.* [16], reported coating of ZnO nanorods on CNTs by chemical vapor deposition (CVD) in a tube furnace. L. Gao *et al.* reported the deposition of ZnO particles on multiwalled CNTs (MWNTs) and enhanced photocatalytic activity [17,18]. In hybrid systems, control of the particle size and interparticle distance are essential to their applications in electronic and photonic devices [2]. In addition, the functionalization of CNTs to anchor nanoparticles will change the surface property of CNTs [17,18]. Hence, the application potential of ZnO nanoparticles on CNT scaffolds needs to be further investigated.

2 EXPERIMENTAL METHODS

Aligned MWNTs were grown on silicon substrates coated with iron nanoparticles using Plasma-Enhanced Chemical Vapor Deposition (PECVD) [19]. CuO nanowires were synthesized via hotplate method [20]. The as-grown MWNTs or CuO nanowires were placed into a RF plasma assisted sputtering system (Denton Discovery-18) to be sputtered with a Zn film under room temperature (20ºC). Ar plasma with a power of about 100 W was induced to bombard a pure Zn (99.9%, Aldrich) target. The deposition durations varied from 1 to 7 minutes. Subsequently, as-sputtered samples were put onto a hotplate and heated at 400 ºC in ambient conditions for 2-3 hours. After cooling down, the as-grown products were characterized by SEM (JEOL JSM-6400F), TEM (Philips CM300 and JEOL FEM-3010F, 300kV), micro-PL spectroscopy (Renishaw). For the measurements of nonlinear optical performance, the MWNTs were grown on quartz substrates and then beaded with ZnO nanoparticles by following the same processes. The laser pulses were generated by a mode-locked Ti: Sapphire laser (Quantronix, IMRA), which seeded a Ti: Sapphire regenerative amplifier (Quantronix, Titan).

3 RESULTS AND DISCUSSION

3.1 Morphology and structure

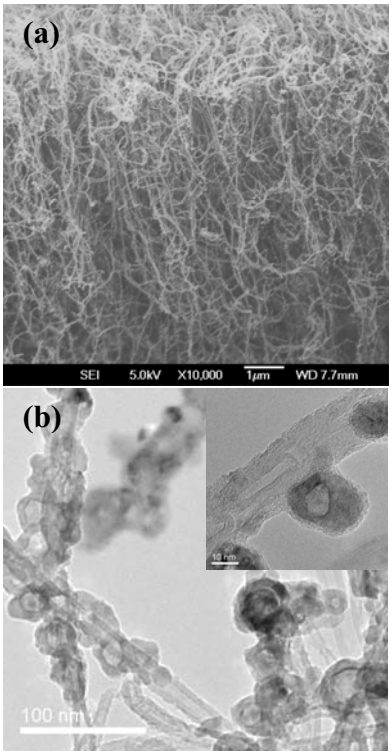

Figure1: (a) Typical SEM image of ZnO/CNTs hybrids after 3min Zn-coating. (b) TEM and (inset) HRTEM images of ZnO nanoparticles anchored on MWNTs.

Figure 1(a) shows the general surface morphology of a ZnO-coated CNT sample. It can be seen that the original smooth MWNTs are decorated by ZnO nanoparticles, forming chain-like structures. Going into the lower part of the CNTs forest, the density of nanoparticles obviously decreases due to the screening of neighboring CNTs. Nearby the surface, the size distribution and the interparticle distance of the ZnO nanobeads could be readily controlled by changing the thickness of the Zn coating. Extended SEM study showed that, with 1min, 3min and 5min of Zn-coating, the average diameter of ZnO nanoparticles increased from 19.2 to 26.2 and 36.6 nm, respectively. For each case, the size distribution of ZnO nanoparticles roughly followed a Gaussian profile. On the other hand, with the increase in coating thickness, the average distance between particles was reduced. Such controllable interaction between adjacent nanoparticles along one dimension is very important to the collective behavior in nanoparticle assembly.

Figure 1(b) shows the typical TEM and high-resolution (HRTEM) images of the sample with 3min Zn-coating. It can be seen that hollow ZnO beads were formed along MWNTs. Such hollow beads were also found in the products from 1min Zn-coating. In Figure 1(b), some cavities in hollow beads appear to follow a polyhedral shape, although the particles do not have a regular shape. From the HRTEM image, the intact MWNT structure and crystalline fringes of ZnO nanoparticles are clearly observed. There is a thin amorphous layer surrounding the whole particle and connecting the wall of the MWNT at the same time. Such compact connection between the MWNT and the ZnO nanoparticle could be due to the good wettability of melted Zn on the surface of CNTs [15]. For the nanoparticle, the lattice spacings and interfacial angle can be characterized to be the hexagonal ZnO structure. However, the tubular CNT wall makes it difficult to epitaxially grow the non-layer-structural ZnO nanoparticle.

3.2 Low Temperature PL

The photoluminescence (PL) spectra at 77K from the samples with different coating thickness are shown in Figure 2(a). With the increase in content of the ZnO nanoparticles, the PL intensity increases. Several main peaks or shoulders were marked by dashed lines to guide the eyes. Compared with PL results under lower temperature (<77K, typically 4.2K) [21], all the bands are quite broad and no sharp peaks can be distinguished. From previous reports on the PL of ZnO [21-23], the band near

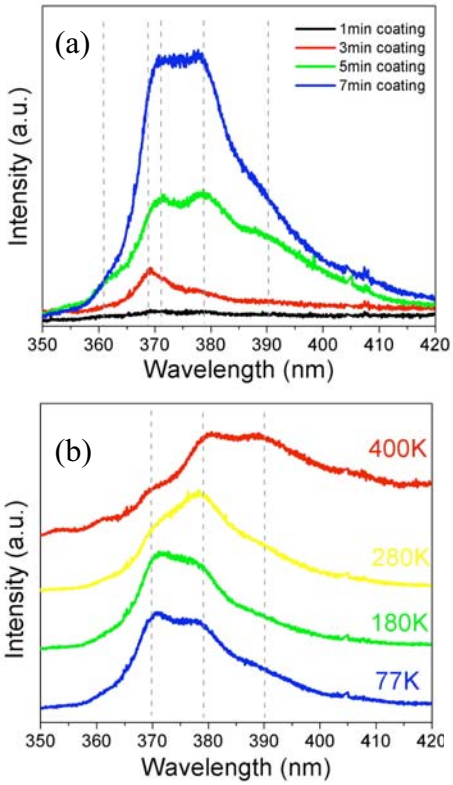

Figure 2: (a) PL spectra of ZnO/CNTs with different coating thickness at the low temperature of 77K. (b) Temperature dependence of PL spectra from the sample with 3min Zn-coating.

361 nm can be ascribed to the free exciton (FX) recombination. And the band at about 369 nm could be due to the bound exciton emission. Relatively, the sample from 3min Zn-coating gives the strongest bound exciton emission. However, the FX (A) and FX (B) can not be distinguished, possibly due to defects in ZnO nanoparticles. The two strong bands at about 372 nm and 378 nm may be related to the first order and second order LO phonon assisted FX emission, respectively, since strong 1LO and 2LO peaks of ZnO were observed in the resonant Raman spectra (no shown) for the same samples. And the shoulder at about 390 nm could also be attributed to the LO–phonon replicas. It is worth noting that with increase in the coating durations, the signal of LO replicas becomes stronger and the original free and bound exciton emission are suppressed. Such a role of phonons could be related to the increasing particle size and decreasing interparticle distance. The strong phonon effects may also involve the effects of CNTs, which connect particles. Furthermore, the two-electron satellite (TES) could be included in the part between 1LO and 2LO bands. Thus the platform for the sample with 7min coating suggests that bigger and continues ZnO nanoparticles may give stronger rediative recombination and high density of donor should be responsible for this [21].

Temperature dependence of the sample with 3min coating is shown in Figure 2(b). It can be seen that, with the increase in the temperature, the main band shift to longer wavelength, similar with previous reports [24,25]. Due to the stronger phonon effects under higher temperature, almost all the peaks mix together and higher order LO replicas dominate. On the other hand, more ionized defects levels would also narrow the band gap of ZnO, which results in a broad band between 380-390 nm, frequently observed from the room temperature PL results.

3.3 Nonlinear optical properties

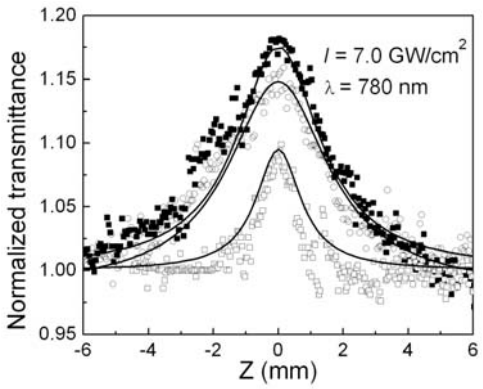

Figure 3: Open aperture Z-scans of the as-grown MWNTs (filled squares) and ZnO-beaded MWNTs with 1min (open circles) and 5min Zn-coating (open squares). The solid lines are the best-fit curves calculated by the Z-scan theory.

Using femtosecond laser pulses at a wavelength of 780 nm, we have observed ultrafast absorptive nonlinearities in films of ZnO nanoparticles beaded MWNTs on quartz substrates. To minimize average power and reduce accumulative thermal effects, 220-fs laser pulses at 1 kHz repetition rate were employed. The laser pulses were focused onto the samples with a minimum beam waist of about 15 mm. The incident and transmitted laser powers were monitored as the samples were moved (or Z-scanned) along the propagation direction of the laser pulses.

Figure 3 displays the typical open-aperture Z-scans, showing negative signs for the absorptive nonlinearity. The Z-scan curve on as-grown MWNTs shows a typical signal for saturable absorption, consistent with our previous report [26]. On the other hand, from ZnO/MWNTs with 1min coating, the transmittance shows only slight reduction, compared with that from as-grown MWNTs. However, for the sample with 5min coating, the normalized transmittance is significantly reduced. Such a reduction is believed to be induced by three-photon absorption in the presence of ZnO nanoparticles. With the total energy of three photons (3 x 1.59 eV), a valence band electron can be excited to the conduction band in ZnO (Eg = 3.37 eV for bulk ZnO). Such a nonlinear process gives rise to a positive contribution to the nonlinear absorption, as contrast to the saturable absorption. As a consequence, the resultant nonlinear absorption is the interplay between the three-photon absorption in ZnO nanoparticles and the saturable absorption in MWNTs. Such interplay provides an effective way to control the nonlinear response by changing the concentration of the ZnO nanoparticles in our ZnO/MWNTs hybrid system.

3.4 ZnO coated CuO nanowires

In our previous work, aligned CuO nanowires have been synthesized by simply heating Cu in ambience on a hotplate. The as-grown CuO nanowires have given very uniform field emission images [20]. By following the same procedures, ZnO nanoparticles were also anchored on the CuO nanowires. Figure 4(a) shows the surface morphology of ZnO-coated CuO nanowire films. Normally, as-grown CuO nanowires have an average diameter of about 60-90 nm and the cylindrical wall is smooth. After 2.5 min Zn-coating and 3h heating, we can see the CuO nanowires are fully covered with nanoparticles and their diameter increases to about 130-150 nm. Different with the situation for CNTs, all nanoparticles on CuO nanowires are connected even for only 2.5min Zn-coating. From the TEM image shown in Figure 4(b), we can see the nanoparticles are closely anchored on the wall of nanowires. Due to the larger diameter of CuO nanowires, ZnO nanoparticles did not form chain-like structures but just adhered on the surface of nanowires. The different wettability property of liquid ZnO for CNTs and CuO would also affect the particle morphology. Further structural study is still in

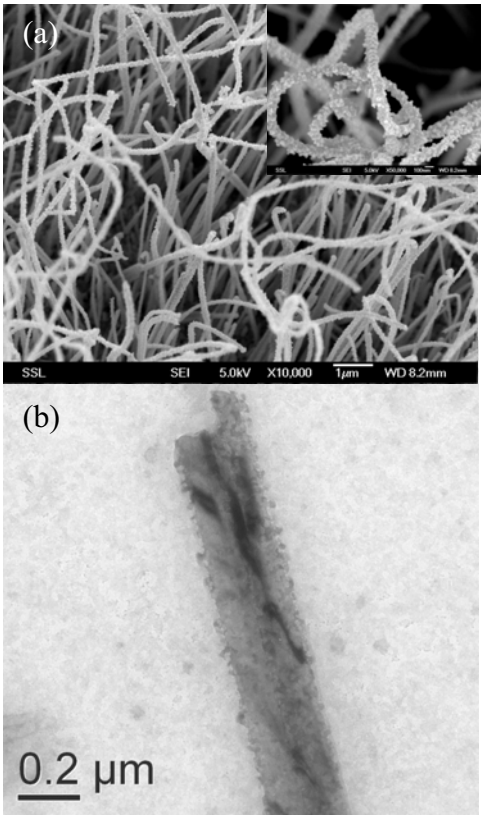

Figure 4: (a) Typical SEM image of ZnO/CuO NWs hybrid structures. Inset shows a high-magnification image. (b) TEM of ZnO nanoparticles on a CuO nanowire stem.

process. Since ZnO itself is a good field emission material [21], the ZnO protrusions may further enhance the field emission properties of CuO nanowires. In addition, since ZnO is intrinsically n-type semiconductor and CuO p-type, a heterojunction may form based on the ZnO/CuO hybrids, which may give interesting photo-electronic property. Moreover, it is expected that the larger specific surface area of ZnO nanoparticles on such CNTs/nanowires forests would further enhance the performance of ZnO as biological catalyst and gas sensor.

4 CONCLUSION

ZnO nanoparticles have been integrated on the CNTs and CuO nanowires by simply annealing Zn-coated as-grown nanotubes/nanowires in ambience. The obtained ZnO nanoparticles are single crystalline, whose size can be readily controlled by the coating thickness. Based on ZnO/CNTs hybrids, low-temperature PL property has been studied and a tunable nonlinear absorption behavior has been demonstrated. Our results highlight opportunities for integrating CNTs/nanowires with other functional oxide nanoparticles via a simple method, and exploring the collective properties of nanoparticles/CNTs or nanowires hybrid materials.

REFERENCES

[1] A. P. Alivisatos, Science 271, 933, 1996.
[2] Z. Tang and N. A. Kotov, Adv. Mater. 17, 951, 2005.
[3] E. C. Walter and B. J. Murray, F. Favier, R. M. Penner, Adv. Mater. 15, 396, 2003.
[4] S. Fullam, D. Cottel, H. Rensmo and D. Fitzmaurice, Adv. Mater. 12, 1430, 2000.
[5] Y. P. Sun, W. Huang, Y. Lin, K. Fu, A. kitaygorodskiy, L. A. Riddle, Y. J. Yu and D. L. Carroll, Chem. Mater. 13, 2864, 2001.
[6] M. Endo, Y. A. Kim, M. Ezaka, K. Osada, T. Yanagisawa, T. Hayashi, M. Terrones and M. S. Dresselhaus, Nano Lett. 3, 723, 2003.
[7] W. Q. Han and A. Zettl, Nano Lett. 3, 681, 2003.
[8] X. Li, J. Niu, J. Zhang, H. Li and Z. Liu, J. Phys. Chem. B 107, 2453, 2003.
[9] F. E. Osterloh, J. S. Martino, H. Hiramatsu and D. P. Hewitt, Nano Lett. 3, 125, 2003.
[10] W. A. de Heer, P. Poncharal, C. Berger, J. Gezo, Z. Song, J. Bettini and D. Ugarte, Science 307, 907, 2005.
[11] J. S. Ye, H. F. Cui, X. Liu, T. M. Lim, W. D. Zhang and F. S. Sheu, Small 1, 560, 2005.
[12] L. Fu, Z. Liu, Y. Liu, B. Han, P. Hu, L. Cao and D. Zhu, Adv. Mater. 17, 217, 2005.
[13] K. C. Chin, A. Gohel, W. Z. Chen, H. I. Elim, W. Ji, G. L. Chong, C. H. Sow and A. T. S. Wee, Chem. Phys. Lett. 409, 85, 2005.
[14] Z. L. Wang, J. Phys.: Condens. Matt. 16, R829, 2004.
[15] H. Kim and W. Sigmund, Appl. Phys. Lett. 81, 2085, 2002.
[16] S. Y. Bae, H. W. Seo, H. C. Choi, J. Park and J. Park, J. Phys. Chem. B 108, 12318, 2004.
[17] J. Sun, L. Gao and M. Iwasa, Chem. Commun. 832, 2004.
[18] L. Jiang and L. Gao, Mater. Chem. Phys. 91, 313, 2005.
[19] Y. H. Wang, J. Lin, C. H. A. Huan and G. S. Chen, Appl. Phys. Lett. 79, 680 2001.
[20] Y. W. Zhu, T. Yu, F. C. Cheong, X. J. Xu, C. T. Lim, V. B. C .Tan, J. T. L. Thong and C. H. Sow, Nanotechnology, 16, 88, 2005.
[21] Ü. Özgür, Ya. I. Alivov, C. Liu, A. Teke, M. A. Reshchikov, S. Doğan, V. Avrutin, S.-J. Cho and H. Morkoçd, J. Appl. Phys. 98, 041301, 2005.
[22] D. W. Hamby, D. A. Lucca, M. J. Klopfstein and G. Cantwell, J. Appl. Phys. 93, 3214, 2003.
[23] K. Thonke, Th. Gruber, N. Teofilov, R. Schönfelder, A. Waag and R. Sauer, Physica B 308-310, 945, 2001.
[24] T. Shimomura, D. Kim, M. Nakayama, J. Lumin. 112, 191, 2005.
[25] Y. W. Chen, Y. C. Liu, S. X. Lu, C. S. Lu, C. L. Shao, C. Wang, J. Y. Zhang, Y. M. Lu, D. Z. Shen, X. W. Fan, J. Chem. Phys. 123, 134701, 2005.
[26] H. I. Elim, W. Ji, G. H. Ma, K. Y. Lim, C. H. Sow and C. H. A. Huan, Appl. Phys. Lett. 85, 1799, 2004.